

## Direct Detection of Radical Cations of NADH Analogues

Shunichi Fukuzumi,\* Osamu Inada, and Tomoyoshi Suenobu

Department of Material and Life Science, Graduate School of Engineering, CREST, JST, Osaka University, Suita, Osaka 565-0871, Japan

Received June 11, 2002

Dihyronicotinamide adenine dinucleotide (NADH) is the most important electron source in the biological redox reactions.<sup>1</sup> NADH and analogues usually act as the source of two electrons and a proton, thus formally transferring a hydride ion to a suitable substrate.<sup>2,3</sup> However, there have been a number of instances where NADH acts as one-electron donor in electron-transfer reactions.<sup>4–8</sup> Gebicki et al. have shown that certain classes of radical cations can undergo spontaneous tautomerization and that such radical cation tautomerization can be expanded for radical cations generated from NADH model compounds as shown in Scheme 1, where 1-benzyl-1,4-dihyronicotinamide (BNAH) is shown as a typical NADH model compound.<sup>9,10</sup> The tautomerization is important in the regeneration of NADH/NAD<sup>+</sup> coenzymes employed as chiral catalysts.<sup>2,3</sup>

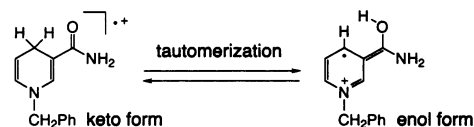
Despite the extremely important role of NADH as an electron source, the direct detection of the one-electron-oxidized species, that is, NADH radical cation or its analogues, has yet to be attained because of the instability of the radical cations. The ESR detection of radical cations of NADH analogues would provide definitive information on the structure of the radical cation as to whether it is the keto form or the enol form.

Here we report the first successful direct detection of radical cations of NADH analogues as the transient absorption spectrum as well as the ESR spectrum in the electron-transfer oxidation of NADH analogues at low temperatures. The ESR spectra clearly indicate that the generated radical cations of NADH analogues are the keto form.

The relatively long lifetime of the radical cation of BNAH enabled us to detect the ESR spectrum for the first time in the electron-transfer oxidation of BNAH with Fe(bpy)<sub>3</sub><sup>3+</sup> in deaerated acetonitrile (MeCN) by applying a rapid-mixing ESR technique as shown in Figure 1a.<sup>11</sup> The *g*-value is 2.0031 which is slightly larger than the free spin value, indicating the contribution of spin–orbit coupling due to electron spin at the nitrogen and oxygen atoms. The hyperfine coupling constants (hfc) are determined by comparison of the observed spectrum with the computer-simulated spectrum as shown in Figure 1b. By comparing the hfc values with the spin densities obtained by the DFT (density functional theory) calculation, the hfc values are assigned as shown in Figure 1b.<sup>12</sup> A large hfc value (53.0 G) is assigned to the two protons at the C(4) position. This clearly indicates that the observed radical cation is the keto form rather than the enol form in Scheme 1.

Deuterium substitution at these positions permits an experimental verification of the assignment of the observed radical species, since a single deuterium gives a triplet (instead of doublet) hyperfine pattern and the deuterium splitting should decrease by the magnetogyric ratio of proton to deuterium (0.153).<sup>13</sup> In fact, deuterium substitution of two hydrogen atoms at the C(4) position of the keto

Scheme 1



form of BNAH<sup>•+</sup> results in drastic changes in the splitting pattern from the spectrum in Figure 1a to that in Figure 1c, where BNAH is substituted by BNAH-4,4'-d<sub>2</sub>. The computer simulation spectrum using the same hfc values except for the deuterium (*I* = 1) at the C(4) position, which are reduced by a factor of 0.153, agrees well with the observed ESR spectrum of the BNAH-4,4'-d<sub>2</sub><sup>•+</sup> (Figure 1d). Such an agreement confirms the hfc assignment in Figure 1.

The dynamics of electron-transfer oxidation of BNAH was also examined using Fe(bpy)<sub>3</sub><sup>3+</sup> as a one-electron oxidant in MeCN. The initial electron transfer from BNAH to Fe(bpy)<sub>3</sub><sup>3+</sup> is too rapid to be monitored using a stopped-flow technique. This is consistent with the largely negative free energy change of electron transfer from BNAH (*E*<sub>ox</sub><sup>0</sup> vs SCE = 0.57 V)<sup>5</sup> to Fe(bpy)<sub>3</sub><sup>3+</sup> (*E*<sub>red</sub><sup>0</sup> vs SCE

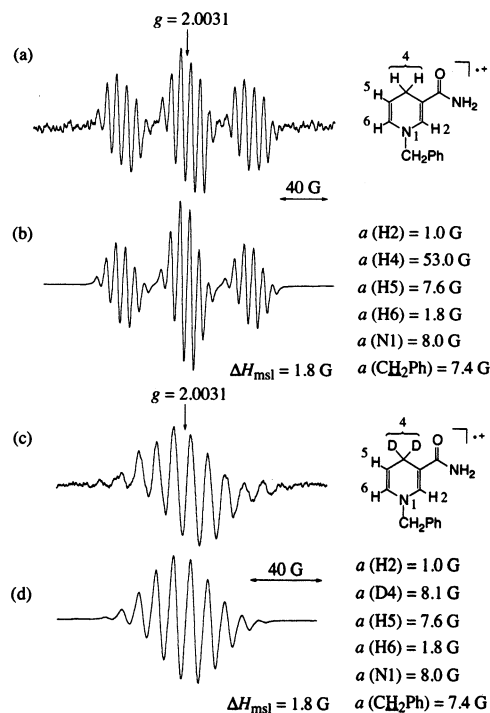


**Figure 1.** (a) ESR spectrum of the keto form of BNAH<sup>•+</sup> generated by oxidation of BNAH ( $8.3 \times 10^{-3}$  M) with Fe(bpy)<sub>3</sub><sup>3+</sup> ( $1.0 \times 10^{-2}$  M) in deaerated MeCN at 233 K and (b) the computer simulation spectrum with the hfc values. (c) ESR spectrum of the keto form of BNAH-4,4'-d<sub>2</sub><sup>•+</sup> generated by oxidation of BNAH-4,4'-d<sub>2</sub> ( $8.3 \times 10^{-3}$  M) with Fe(bpy)<sub>3</sub><sup>3+</sup> ( $1.0 \times 10^{-2}$  M) in deaerated MeCN at 233 K and (d) the computer simulation spectrum with the hfc values.

\* To whom correspondence should be addressed. E-mail: fukuzumi@ap.chem.eng.osaka-u.ac.jp.

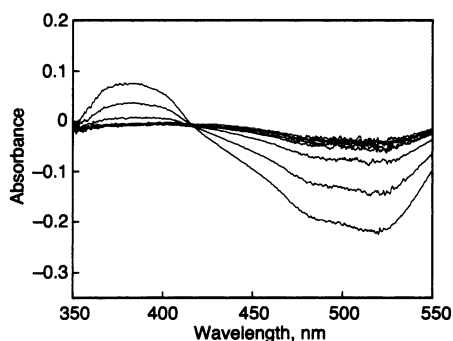
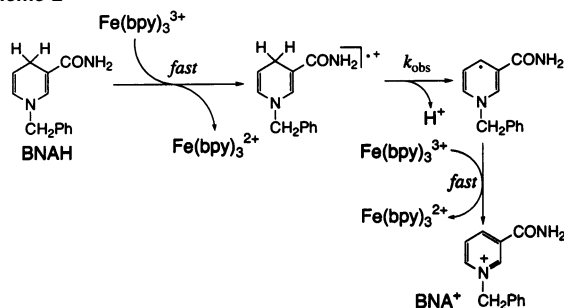


**Figure 2.** Differential spectral change in thermal electron transfer from BNAH ( $1.0 \times 10^{-4}$  M) to  $\text{Fe}(\text{bpy})_3^{3+}$  ( $1.5 \times 10^{-4}$  M) in deaerated MeCN at 298 K; time interval 20 ms.

### Scheme 2



= 1.06 V).<sup>14</sup> The differential absorption spectra were recorded by subtracting the final absorption spectrum from the observed spectra during the electron-transfer reaction as shown in Figure 2. The new absorption band at 380 nm appears upon mixing MeCN solutions of BNAH and  $\text{Fe}(\text{bpy})_3^{3+}$  and disappears, accompanied by the appearance of the absorption band at 520 nm due to  $\text{Fe}(\text{bpy})_3^{2+}$ . The absorption band at 380 nm can be assigned to  $\text{BNAH}^{+\bullet}$ . The decay rate of the  $\text{BNAH}^{+\bullet}$  obeys first-order kinetics, coinciding with the rate of formation of  $\text{Fe}(\text{bpy})_3^{2+}$ . When BNAH is replaced by BNAH-4,4'-*d*<sub>2</sub>, the kinetic isotope effects ( $k_{\text{H}}/k_{\text{D}} = 1.9$  at 243 K) were observed for both the decay rate of  $\text{BNAH}^{+\bullet}$  and the rate of formation of  $\text{Fe}(\text{bpy})_3^{2+}$ .<sup>15,16</sup> This indicates that the decay of  $\text{BNAH}^{+\bullet}$  occurs via deprotonation to produce  $\text{BNA}\cdot$  which is rapidly oxidized by  $\text{Fe}(\text{bpy})_3^{2+}$  as shown in Scheme 2. The Eyring plot of the deprotonation afforded the activation parameters for  $\text{BNAH}^{+\bullet}$  ( $\Delta H^\ddagger = 3.1$  kcal mol<sup>-1</sup>,  $\Delta S^\ddagger = 42$  cal K<sup>-1</sup> mol<sup>-1</sup>) and  $\text{BNAH-4,4'-d}_2^{+\bullet}$  ( $\Delta H^\ddagger = 4.1$  kcal mol<sup>-1</sup>,  $\Delta S^\ddagger = 39$  cal K<sup>-1</sup> mol<sup>-1</sup>).<sup>17</sup> Judging from the highly negative oxidation potential of  $\text{BNA}\cdot$  ( $E_{\text{ox}}^0$  vs SCE = -1.08 V),<sup>5</sup> which is equivalent to the reduction potential of  $\text{BNA}^+$ , the electron transfer from  $\text{BNA}\cdot$  to  $\text{Fe}(\text{bpy})_3^{2+}$  ( $E_{\text{red}}^0$  vs SCE = 1.06 V) is highly exergonic, and thus it is expected to be diffusion-limited. In such a case, the rate-limiting step for formation of  $\text{Fe}(\text{bpy})_3^{2+}$  is the deprotonation from  $\text{BNAH}^{+\bullet}$  as observed experimentally.

When BNAH is replaced by 4-*t*-BuBNAH where the hydrogen at C(4) position is substituted by *tert*-butyl group, no transient absorption spectrum due to *t*-BuBNAH<sup>+</sup> has been detected. One-electron oxidation of *t*-BuBNAH is known to result in the selective C(4)–C bond cleavage of *t*-BuBNAH<sup>+</sup> to give *t*-Bu• and  $\text{BNA}^+$ ,<sup>8b,18</sup> both of which have no absorption bands in the visible region. In such a case, two-electron oxidation of *t*-BuBNAH occurs with 2 equiv of  $\text{Fe}(\text{bpy})_3^{3+}$ . The second electron transfer from *t*-Bu• ( $E_{\text{ox}}^0$  vs SCE = 0.09 V),<sup>19</sup> which is generated via the facile C–C bond

cleavage in *t*-BuBNAH<sup>+</sup>, to  $\text{Fe}(\text{bpy})_3^{3+}$  ( $E_{\text{red}}^0$  vs SCE = 1.06 V) is as rapid as the initial electron transfer from *t*-BuBNAH ( $E_{\text{ox}}^0$  vs SCE = 0.71 V)<sup>18</sup> to  $\text{Fe}(\text{bpy})_3^{3+}$ .<sup>20</sup>

**Acknowledgment.** This work was partially supported by Grants-in-Aid for Scientific Research on Priority Area (Nos. 13440216, 13750760, and 14045249) from the Ministry of Education, Culture, Sports, Science and Technology, Japan.

**Supporting Information Available:** Data for the transient absorption spectrum of  $\text{BNAH}^{+\bullet}$ , the kinetic data, and the DFT calculation (PDF). This material is available free of charge via the Internet at <http://pubs.acs.org>.

### References

- (1) Stryer, L. *Biochemistry*, 3rd ed; Freeman: New York, 1988; Chapter 17.
- (2) (a) Eisner, U.; Kuthan, J. *Chem. Rev.* **1972**, *72*, 1. (b) Stout, D. M.; Meyers, A. I. *Chem. Rev.* **1982**, *82*, 223.
- (3) (a) Kreevoy, M. M.; Ostović, D.; Lee, I.-S. H.; Binder, D. A.; King, G. W. *J. Am. Chem. Soc.* **1988**, *110*, 524. (b) Kim, Y.; Truhlar, D. G.; Kreevoy, M. M. *J. Am. Chem. Soc.* **1991**, *113*, 7837. (c) Lee, I.-S. H.; Jeoung, E. H.; Kreevoy, M. M. *J. Am. Chem. Soc.* **1997**, *119*, 2722.
- (4) (a) Fukuzumi, S.; Tanaka, T. *Photoinduced Electron Transfer*; Fox, M. A.; Chanon, M., Eds.; Elsevier: Amsterdam, 1988; Part C, Chapter 10. (b) Fukuzumi, S. *Advances in Electron-Transfer Chemistry*; Mariano, P. S., Ed.; JAI Press: Greenwich, CT, 1992; pp 67–175. (c) He, G.-X.; Blasko, A.; Bruce, T. C. *Bioorg. Chem.* **1993**, *21*, 423.
- (5) (a) Fukuzumi, S.; Koumitsu, S.; Hironaka, K.; Tanaka, T. *J. Am. Chem. Soc.* **1987**, *109*, 305. (b) Fukuzumi, S.; Kondo, Y.; Tanaka, T. *J. Chem. Soc., Perkin Trans. 2* **1984**, 673. (c) Fukuzumi, S.; Ohkubo, K.; Tokuda, Y.; Suenobu, T. *J. Am. Chem. Soc.* **2001**, *122*, 4286.
- (6) (a) Powell, M. F.; Bruce, T. C. *J. Am. Chem. Soc.* **1983**, *105*, 1014, 7139. (b) Chipman, D. M.; Yaniv, R.; van Eikeren, P. *J. Am. Chem. Soc.* **1980**, *102*, 3244. (c) Almarsson, Ö.; Sinha, A.; Gopinath, E.; Bruce, T. C. *J. Am. Chem. Soc.* **1993**, *115*, 7093.
- (7) (a) Ohno, A.; Ishikawa, Y.; Yamazaki, N.; Okamura, M.; Kawai, Y. *J. Am. Chem. Soc.* **1998**, *120*, 1186. (b) Pestovsky, O.; Bakac, A.; Espenson, J. H. *J. Am. Chem. Soc.* **1998**, *120*, 13422. (c) Carlson, B. W.; Miller, L. L. *J. Am. Chem. Soc.* **1985**, *107*, 479.
- (8) (a) Anne, A.; Fraoura, S.; Grass, V.; Moiroux, J.; Savéant, J.-M. *J. Am. Chem. Soc.* **1998**, *120*, 2951. (b) Anne, A.; Moiroux, J.; Savéant, J.-M. *J. Am. Chem. Soc.* **1993**, *115*, 10224. (c) Anne, A.; Hapiot, P.; Moiroux, J.; Neta, P.; Savéant, J.-M. *J. Am. Chem. Soc.* **1992**, *114*, 4694.
- (9) Gebicki, J.; Bally, T. *Acc. Chem. Res.* **1997**, *30*, 477.
- (10) (a) Marcinek, A.; Adamus, J.; Huben, K.; Gebicki, J.; Bartczak, T. J.; Bednarek, P.; Bally, T. *J. Am. Chem. Soc.* **2000**, *122*, 437. (b) Marcinek, A.; Rogowski, J.; Adamus, J.; Gebicki, J.; Bednarek, P.; Bally, T. *J. Phys. Chem. A* **2000**, *104*, 718.
- (11) The ESR measurements were performed on a JEOL JES-FA100 ESR spectrometer using a JEOL ES-EMCNT1 rapid mixing flow apparatus. The ESR spectra were recorded under nonsaturating microwave power conditions. The magnitude of modulation was chosen to optimize the resolution and the signal-to-noise (S/N) ratio of the observed spectra.
- (12) The assignment of the hfc values is made by comparison with the hfc values predicted by the DFT calculation. Density-functional theory (DFT) calculations were performed on a COMPAQ DS20E computer. Geometry optimizations were carried out using the B3LYP functional and 6-31G<sup>+</sup> basis set with the unrestricted Hartree–Fock (UHF) formalism as implemented in the Gaussian 98 program. The calculated hfc values are used for assignment of the observed hfc values (see Supporting Information).
- (13) Wertz, J. E.; Bolton, J. R. *Electron Spin Resonance Elementary Theory and Practical Applications*; McGraw-Hill: New York, 1972.
- (14) Fukuzumi, S.; Nakanishi, I.; Tanaka, K.; Suenobu, T.; Tabard, A.; Guillard, R.; Caemelbecke, E. V.; Kadish, K. M. *J. Am. Chem. Soc.* **1999**, *121*, 785.
- (15) The  $k_{\text{H}}/k_{\text{D}}$  value (1.9) is similar to the maximum value reported for proton transfer from  $\text{BNAH}^{+\bullet}$  to bases (2.0),<sup>5b</sup> but significantly smaller than the value (9.0) reported for the deprotonation of the radical cation of 10-methyl-9,10-dihydroacridine ( $\text{AcrH}_2^{+\bullet}$ )<sup>16</sup> probably due to the larger p*K*<sub>a</sub> value of  $\text{BNAH}^{+\bullet}$  than that of  $\text{AcrH}_2^{+\bullet}$ .<sup>5a</sup>
- (16) Fukuzumi, S.; Tokuda, Y.; Kitano, T.; Okamoto, T.; Otera, J. *J. Am. Chem. Soc.* **1993**, *115*, 8960.
- (17) Only the keto form was detected at 243–298 K.
- (18) (a) Fukuzumi, S.; Suenobu, T.; Patz, M.; Hirasaka, T.; Itoh, S.; Fujitsuka, M.; Ito, O. *J. Am. Chem. Soc.* **1998**, *120*, 8060. (b) Takada, N.; Itoh, S.; Fukuzumi, S. *Chem. Lett.* **1996**, 1103.
- (19) Wayner, D. D. M.; McPhee, D. J.; Griller, D. *J. Am. Chem. Soc.* **1988**, *110*, 132.
- (20) The two electron oxidation mechanism of *t*-BuBNAH including the trap of *t*-Bu• radical with oxygen has previously been reported. See ref 18b.

JA0272538